

# RHESSI investigation of solar flare footpoints

T. Mrozek \*

*Astronomical Institute, University of Wrocław, ul. Kopernika 11, 51-622 Wrocław, Poland*

Received 27 April 2005; received in revised form 11 July 2006; accepted 5 September 2006

---

## Abstract

Footpoints of several strong solar flares have been investigated using images obtained by Ramaty High Energy Solar Spectroscopic Imager (*RHESSI*). The altitude of hard X-ray sources in various energy bands has been measured. Some observational characteristics of the energy-height relation have been obtained and presented in the form of histograms. Using them we were able to conclude that during impulsive phase the region in which electrons are stopped is rather narrow with the thickness in the range 1500–4000 km. Moreover, it is shown that all electrons producing photons with energies exceeding 20–30 keV are stopped at similar altitudes. For the flare of 3 August 2002 we analysed the temporal evolution of the energy-height relation. It has been shown that changes in this relation can be interpreted as a manifestation of simultaneous upflows and downflows of the transition region and chromosphere. Obtained values of velocities are between –50 and 150 km/s.

© 2006 COSPAR. Published by Elsevier Ltd. All rights reserved.

*Keywords:* Sun; Solar flares; Footpoints; Hard X-rays

---

## 1. Introduction

The thick-target model (Brown, 1971) gives an easy explanation of observed characteristics of the impulsive phase of solar flares. In this model we assume that electrons are accelerated in the top of the flaring loop. Next, they propagate along field lines and reach the chromosphere where they deposit their energy due to Coulomb collisions. During this process we observe the hard X-ray bremsstrahlung and the thermal reaction of the plasma in soft X-rays, UV and white light. Generally, this thermal reaction depends on the energy of propagating electrons. More energetic particles produce the reaction in denser parts of the chromosphere.

The thick-target model predicts that a relation between the energy of hard X-ray sources and their position along the flux tube, i.e. the energy-height relation, should exist. Such an effect has been observed by YOHKOH (Matsushita et al., 1992) and has been theoretically modeled by Fletcher (1996). The first attempt to study the

energy-height relation, using *RHESSI* data, has been already made (Aschwanden et al., 2002; Brown et al., 2002).

In this paper we present an attempt to the statistical analysis of the energy-height relation on the basis of 12 flares observed by *RHESSI*. For strong hard X-ray bursts we were able to study a temporal evolution of this relation.

## 2. Analysis

In our analysis we used data from the *RHESSI* satellite (Lin et al., 2002). We have chosen several strong flares located far from the Sun center (the radial distance greater than 800'') for minimizing the projection effect. The impulsive phases were well observed by *RHESSI* and the footpoints were clearly seen. Selected flares are presented in Table 1.

We adopted the data analysis performed by Aschwanden et al. (2002) with several modifications as follows. For each flare we have chosen a time interval covering the strongest hard X-ray burst and for this time interval we have made images, using the CLEAN algorithm (Högbom, 1974), in different energy ranges with intervals changing from 2 to 20 keV in dependence of photon counts

---

\* Tel.: +48 608057952.

E-mail address: [mrozek@astro.uni.wroc.pl](mailto:mrozek@astro.uni.wroc.pl)

Table 1  
List of investigated flares

(1)	(2)	(3)	(4)	(5)	(6)	(7)	(8)
1	20-FEB-02	11:02	11:07	11:12	C7.5	N16W80	937
2	14-APR-02	22:22	22:29	22:33	C7.2	N19W79	946
3	13-MAY-02	17:40	17:45	17:49	C2.3	S20W86	946
4	29-JUN-02	09:27	09:33	09:37	C2.0	S17E89	946
5	03-AUG-02	18:59	19:07	19:11	X1.0	S15W83	941
6	20-SEP-02	09:21	09:28	09:33	M1.8	S25E76	940
7	04-DEC-02	22:41	22:49	22:57	M2.5	N14E63	871
8	26-APR-03	00:51	00:58	01:00	M2.1	N19W66	892
9	27-APR-03	15:27	15:32	15:35	M1.7	N19W81	946
10	01-NOV-03	22:26	22:38	22:49	M3.2	S14W61	865
11	03-NOV-03	09:43	09:55	10:19	X3.9	N09W74	929
12	04-NOV-03	19:29	19:50	20:06	X28.0	S21W88	973

(1), number of event; (2), date; (3)–(5), start, peak and end times [UT], respectively; (6), GOES class; (7), location; (8), radial distance from the Sun center [“].

statistic. These energy ranges have been shifted by several keV in dependence of the energy range length, i.e. the shift is equal to the half of the energy range length. This gives us energy ranges which have small influence from neighboring intervals and can be treated as almost independent.

The set of images obtained in different energy ranges has been used for the further analysis. For each footpoint we determined the location of its centroid and measured its distance from the level defined by centroids of footpoints obtained for highest energy range (see Fig. 1, left panel). Using a distance from this level, instead of measuring distance from the Sun center, we minimize additional errors which could occur when the flaring structures have other, than parallel, orientations to the solar limb.

Usually, the strong correlation between the hard X-ray source altitude above defined level and its energy has been observed. Centroids of high-energy sources were located systematically lower in the chromosphere than the low-energy ones. An example of such behaviour is presented in Fig. 1 (right panel). Horizontal lines represent the energy

intervals and vertical ones are errors calculated in the height measurements.

Imaging parameters for different energy intervals are identical, i.e. they do not affect relative positions of centroids. The accuracy of the centroid location can be estimated as follows. Each point  $(x_k, y_k)$  of the source has errors  $(\Delta x_k, \Delta y_k)$  connected with the angular resolution. Bogachev et al. (2005) calculated how these errors propagate in the centroid location  $(x_0, y_0)$  and obtained following formula (the same result is for  $\Delta y_0$ ):

$$(\Delta x_0)^2 = \frac{(\Delta x)^2}{n} + \frac{\sum_{k=1}^n (x_k - x_0)^2}{I_0 n^2} \quad (1)$$

where  $\Delta x_0$  is the error in the centroid,  $n$  is the number of pixels in the source and  $I_0$  is the integral intensity of the source. This method was used for HXT images but can be easily adopted for RHESSI images assuming that the angular resolution is determined by the finest grid used for the image reconstruction.

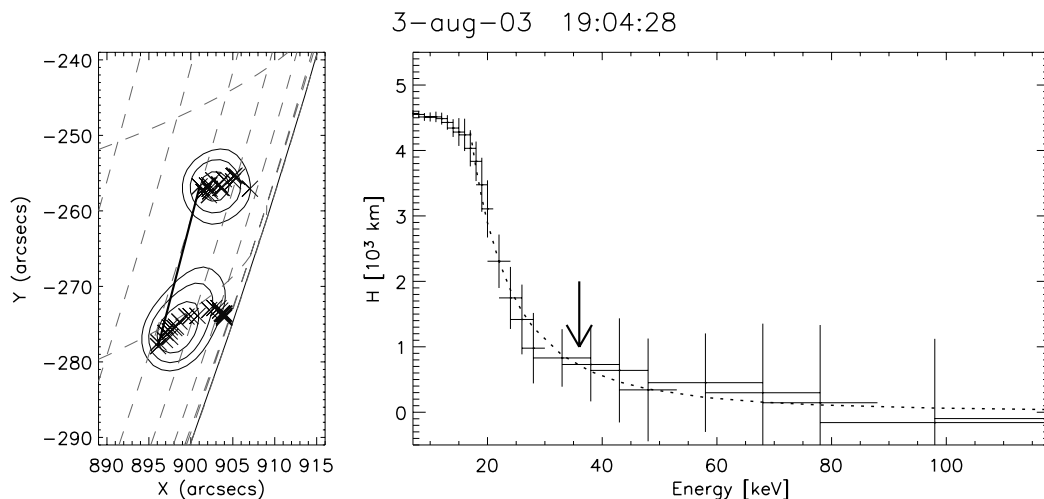


Fig. 1. Left panel: contours, RHESSI 25–35 keV image obtained during the impulsive phase; crosses, locations of centroids of hard X-ray sources obtained for different energies but for the same time; right panel: altitude of centroids above the reference level, the power-law function fit is presented with dotted line. The flattening-point is marked by an arrow.

In Fig. 1 (right panel) we present an example of the power-law function fitted to the observed relation. Points which do not show the change of height with the energy at low energies were skipped from the fitting because in low energies we do not observe double-footpoint morphology. Aschwanden et al. (2002) proposed the power-law function because it is analytically most convenient and gives similar results as the logarithmic or exponential functions. The power-law function fit, which is marked by dotted line, has been used for obtaining some observational characteristics of the energy-height relation. We defined the flattening point as a place where the derivative of the fit is less than 1.45. This value has been chosen arbitrarily for defining qualitatively the point in which the observed relation changes from steep to flat. If we assume that the energy-height relation resembles the column density in the flux tube then the steep part is connected to low density region and the flat part occurs when density drastically rises. The thickness of the region in which electrons deposit their energy due to Coulomb collisions has been assumed as a difference between the maximal and the minimal altitude of centroid positions observed in each footpoint. Such a definition, based on centroids, gives a low limit of the actual value because sources have a certain radial extent which is especially important in low energies.

The analysis is made under some geometrical assumptions concerning important parameters of the loop. The first one is the inclination angle of the loop plane with the respect to the vertical of the solar surface. We assume that the inclination is close to  $0^\circ$ . Otherwise, our estimations of the height will be overestimated or underestimated depending on the positive or negative inclination. However, in the statistical analysis based on the great number of events we should obtain, on the average, results close to actual ones. For these reasons our assumption that loop should be almost perpendicular to the solar surface is

strong but can be weakened by the number of analysed events. The next important parameter is the azimuth angle between the loop footpoint baseline and the heliographic east–west direction. If this parameter is close to the value of 0 then, for close-to-limb flare, footpoints seen in HXR can overlap giving one source with strong radial extension. We analysed two of such events and obtained parameters of the energy-height relations close to the mean values. We verified geometry of analysed flares by comparing RHESSI images with images obtained by TRACE (EUV filters) in the late phase of a flare. Such observations were available for the majority of investigated flares.

### 3. Results

Altogether we obtained 27 energy-height relations for flares listed in Table 1. For each of them we determined the height and the energy of the flattening point and the centroid height range. Results are presented in Fig. 2 in the form of histograms.

The histogram presenting the energy of the flattening point (Fig. 2, left panel) shows that for the majority of events this parameter occurs below 40 keV. Values presented in this histogram have been obtained for different flares and for different stages of the impulsive phase. However, they have low dispersion which means that the chromosphere has a relatively similar density during electron beam precipitation. There are several cases in which we observe the flattening point in energies above 50 keV. Usually, such events have the energy-height relation with two flattening points. The first one occurs in the range of 20–40 keV, next the energy-height relation is rather flat but in the range of 50–80 keV we observe another decrease of the centroids height. An illustration of this behaviour is presented in Fig. 3.

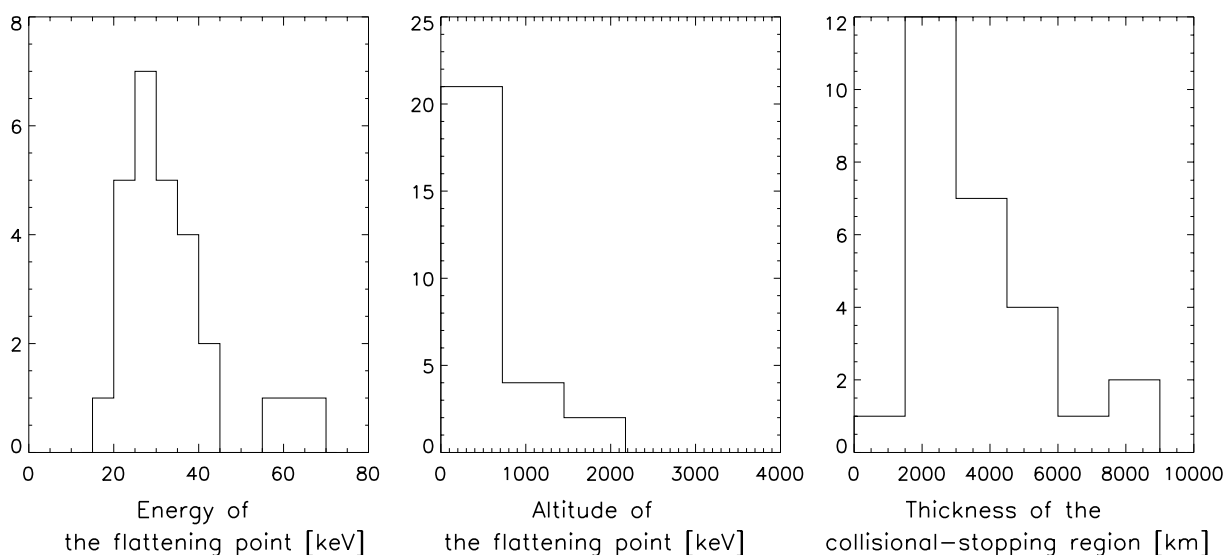


Fig. 2. Histograms of the energy of the flattening point, the altitude of the flattening point and the centroid height range obtained from 27 investigated energy-height relations.

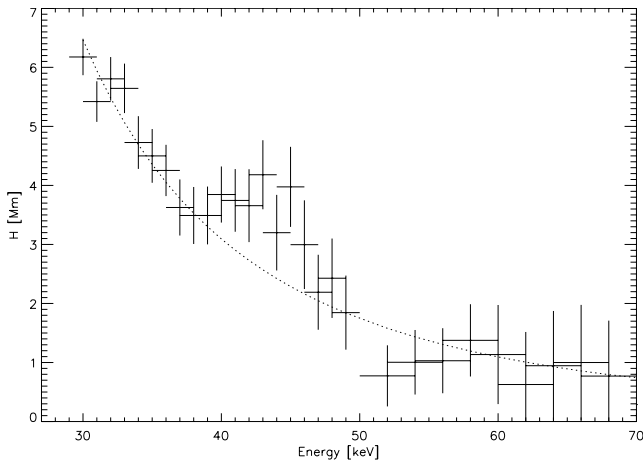


Fig. 3. An example of divergence from the power-law of the energy-height relation observed in the 3 November 2003 flare.

Remembering that the energy-height relation resembles the column density, we can conclude that this is an effect connected with the complexity of the density structure of the chromosphere. For example, Emslie and Nagai (1984) modeled gas dynamics in the impulsive phase and showed that in the chromosphere heated by nonthermal electrons we can expect heterogeneity in the density when upward and downward moving plasma appears at some level. In such a case the column density

will show deviation from smooth (like power-law) shape. Second explanation of the shape seen in Fig. 3 is based on the fact that possibly we observe two footpoints with different energy spectra. Thus, in lower energies only the first footpoint is clearly visible whereas, in higher energies we observe the second footpoint which has the flatter energy spectrum. Other processes like photospheric albedo, mirroring of electrons, return currents and many other could also play a role in producing energy-height relation with two flattening points. For now we are not able to distinguish which of these processes is most important. It will be possible if we calculate detailed models of the energy-height relation. The work is in progress.

Next histogram (Fig. 2, middle panel) presents altitudes of the flattening point. They are relatively low, almost all points show values less than 1500 km above the reference level defined as a high-energy asymptote of the power-law fit.

Electrons are stopped in a relatively narrow region. In the histogram presenting obtained centroid height range (Fig. 2, right panel) about 70% of events have values between 1500 and 4000 km. It can be treated as a typical thickness of the region in which electrons are stopped due to Coulomb collisions. These values are comparable with the typical thickness of the chromosphere.

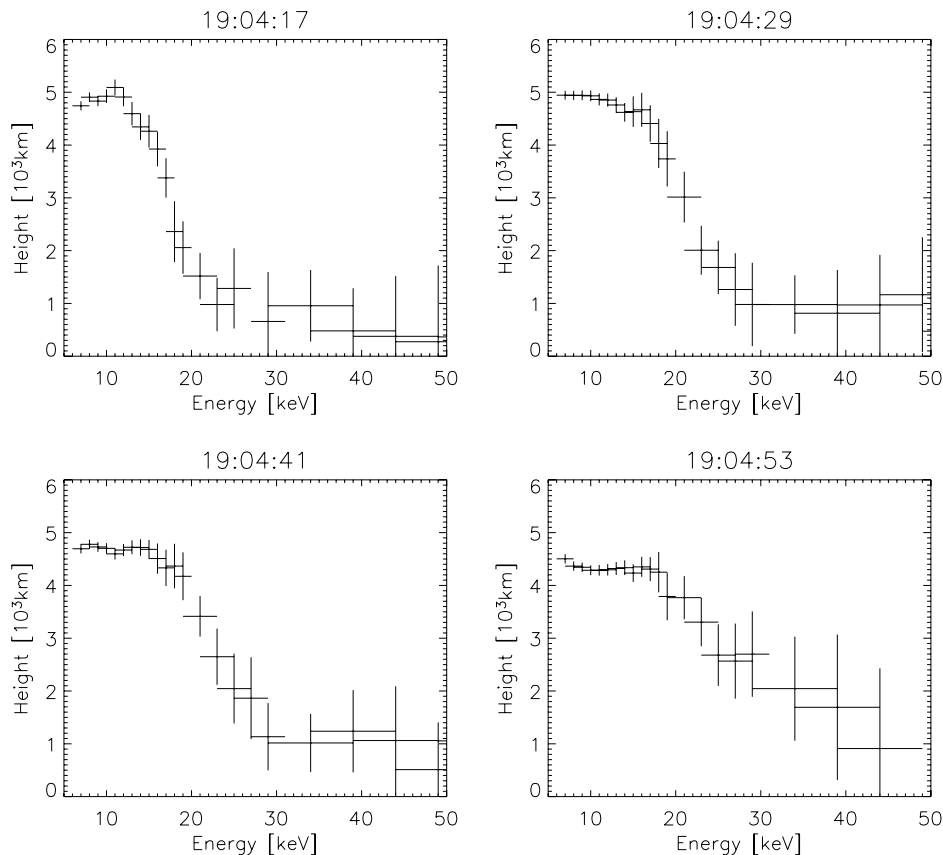


Fig. 4. An example of time evolution of the energy-height relation obtained for the flare of 3 August 2002.

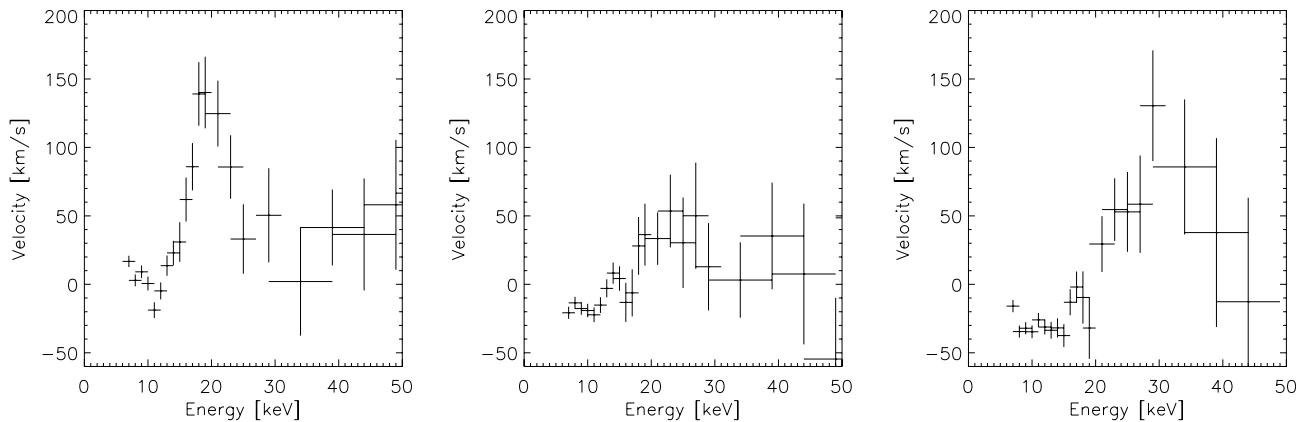


Fig. 5. An example of velocities in the function of the energy obtained for the 3 August 2002 flare.

For one event, the flare of 3 August 2002, we were able to obtain energy-height relations for several consecutive time intervals. The result is presented in Fig. 4. We can see that basic characteristics of the energy-height relation are changing with time. Within observed hard X-ray burst steep part moves up in energies. We treated this effect as some evidence of a systematical change in the density due to the chromospheric evaporation. Energy deposited by electrons in the transition region and the chromosphere was high enough to produce the pressure gradient causing the evaporation. Due to this process the column density changes and we observe that electrons are stopped at higher levels.

We estimated the velocities of the observed changes by subtracting energy-height relations obtained for consecutive intervals. The example of the velocity-energy relation is presented in Fig. 5. This is not exactly the velocity of the moving plasma, but rather the velocity of changes in the chromosphere and transition region density structure. The obtained values are between  $-50$  and  $150$  km/s. Such a range of values suggests that during impulsive phase we observe simultaneously upflows and downflows of plasma in the transition region and chromosphere. The obtained values of the velocity are in a good agreement with the recent results reported by Teriaca et al. (2003).

#### 4. Conclusions

Using the *RHESSI* images we have analysed relation between the location of footpoint hard X-ray sources and their energy. As was reported in former papers (Matsushita et al., 1992; Aschwanden et al., 2002) this relation is clearly visible for limb flares. Our investigation is based on the large set of data, thus we were able to obtain some general characteristics of the energy-height relation i.e. the energy and the altitude of the flattening point and the thickness of the electron-stopping region.

For the majority of events we observe that the energy-height relation becomes flat for energies exceeding  $40$  keV. It means that all electron beams, responsible for producing this radiation, take place at similar altitudes.

The flattening point occurs in the range of  $20$ – $35$  keV and at altitudes below  $1500$  km. Obtained values have low dispersion which means that during electron beams occurrence the chromosphere shows the relatively similar density for different flares.

For several energy-height relations we observed two flattening points at two different altitudes. These events will be analysed further for distinguishing between two interpretations of such behaviour: the complex structure of the chromospheric density or the manifestation of two unresolved footpoints with different energy spectra.

Another important characteristic is the thickness of the region in which we observe hard X-ray emission due to electron beams. The obtained values are between  $1500$  and  $4000$  km which is comparable with typical values of the chromospheric thickness.

For the 3 August 2002 flare we were able to study temporal evolution of the energy-height relation. Assuming, that the relation is caused only by the chromospheric density structure, we have opportunity for studying the early phase of the chromospheric evaporation. Observed changes (Fig. 4) suggest that during electron beams there is a complex evolution in the density structure. We observe, simultaneously, downflows and upflows. The obtained values of the velocity changes from  $-50$  to  $150$  km/s and are in a good agreement with the results reported by Teriaca et al. (2003).

#### Acknowledgments

First, I wish to thank the *RHESSI* Team for the really hard work and dedication, which has made this research possible. I acknowledge many useful and inspiring discussions of Professor M. Tomczak and Doctor S. Kołomański. This investigation has been supported by Grant No. 2 P03D 001 23 from the Polish Committee for Scientific Research (KBN).

## References

- Aschwanden, M.J., Brown, J.C., Kontar, E.P. Chromospheric height and density measurements in a solar flare observed with *RHESSI*. II. Data analysis. *Solar Phys.* 210, 383–405, 2002.
- Bogachev, S.A., Somov, B.V., Kosugi, T., Sakao, T. The motions of the hard X-ray sources in solar flares: images and statistics. *Astrophys. J.* 630, 561–572, 2005.
- Brown, J.C. The deduction of energy spectra of non-thermal electrons in flares from the observed dynamic spectra of hard X-ray bursts. *Solar Phys.* 18, 489, 1971.
- Brown, J.C., Aschwanden, M.J., Kontar, E.P. Chromospheric height and density measurements in a solar flare observed with *RHESSI*. I. Theory. *Solar Phys.* 210, 373–381, 2002.
- Emslie, A.G., Nagai, F. Gas dynamics in the impulsive phase of solar flares. I – Thick-target heating by nonthermal electrons. *Astrophys. J.* 279, 896–908, 1984.
- Fletcher, L. The height distribution of non-thermal X-ray sources in impulsive solar flares. *Astron. Astrophys.* 310, 661–671, 1996.
- Högbom, J.A. Aperture synthesis with a non-regular distribution of interferometer baselines. *Astron. Astrophys.* 15, 417–426, 1974.
- Lin, R.P., Dennis, B.R., Hurford, G.J., et al. The Reuven Ramaty High-Energy Solar Spectroscopic Imager (*RHESSI*). *Solar Phys.* 210, 3–32, 2002.
- Matsushita, K., Masuda, S., Kosugi, T., Inada, M., Yaji, K. Average height of hard X-ray sources in solar flares. *Publ. Astron. Soc. Jpn* 44, L89–L93, 1992.
- Teriaca, L., Falchi, A., Cauzzi, G., et al. *Solar and Heliospheric Observatory/Coronal Diagnostic Spectrograph* and ground-based observations of a two-ribbon flare: spatially resolved signatures of chromospheric evaporation. *Astrophys. J.* 588, 596–605, 2003.